euspen's 23rd International Conference & Exhibition, Copenhagen, DK, June 2023
www.euspen.eu

Edge detection and surface inspection for roll-to-roll and slot-die coating based on machine vision approach

Mothana Hassan[1], Liam Blunt[1], Hussam Muhamedsalih[1]

[1]*EPSRC Future Metrology Hub/ Centre for Precision Technologies (CPT), University of Huddersfield UK*

M.hassan@hud.ac.uk

Abstract

Roll to roll (R2R) processes are critical in the mass production of thin film products especially in flexible electronics. Slot-die techniques is widely used in R2R as a simple but accurate method of applying conducting thin film inks onto a large area flexible substrate. For example, organic conducting inks can be printed directly in the form of tracks with high homogeneity and uniformity. Furthermore, slot-die coating process can potentially be optimised if a sufficient control system is provided, which provides a direct link between the slot-die head and the operating conditions, such as flow-rate of the ink and the speed of the substrate. In this work, the authors are aiming to provide the basis of a feedback system through a machine vision surface inspection system. A method is presented for edge detection to extract quantitative information related to the printed ink edge consistency and hence track width regularity. Monochrome cameras illuminated by a broadband light source are used to captures image frames while the substrate is moving. Different printed ink samples on polymer based substrates have been considered for developing the test protocol. The images are captured at full-bright field, where the substrate is positioned coaxially. A Sobel operator has been used to analyse the captured images in order to inspect coating quality and detect defects, whilst an Otsu's thresholding approach is used to define and extract the edge line of the coating. In this paper, the authors use the lateral arithmetic average (equivalent to R_a parameter in surface metrology) to describe the edge regularity along the printed track. It was found that for the measured tracks, the edge straightness can vary by 0.51 µm ($R_{a(LAT)}$). This metric value can be used as a feedback signal to the control system to adjust the operational conditions during the printing operation.

Slot-die roll-to-roll printed coating inspection, edge detection and evaluation, defect detection, machine vision.

1. Introduction

The roll-to-roll (R2R) manufacturing process is a subject of interest due to its low cost and large production capability. Advanced R2R printing technology focuses on the manufacture flexible electronic components, such as printed sensors, polymer solar cells (OPV), organic photovoltaics (VPO), radio frequency identification (RFID tag), organic light emitting diodes (OLEDS) etc. The ability to make large quantities of such products quickly by using a print line is an attractive feature for many manufacturers [1,2]. As a result, this method has been widely adopted in the manufacture of a range of electronic devices.

The method uses a large-area substrate sheet (usually polymer based) and a variety of printing or coating processes, including ALD coating, spray coating, and commonly slot-die coating printing technologies [3,4]. Due to its high throughput, low cost, minimal material waste and advantageous production speed, the slot-die coating is the most widely used choice for applications in mass-production of various electronic devices [5,6]. In recent years, numerous publications have documented the development of very effective large area coated OPVs and OLEDS on webs such as polyethylene terephthalate (PET) film. However, despite all these advances, there are still a number of practical challenges that need to be overcome in order to more fully exploit R2R technologies [7-9]. In slot-die printing a high aspect ratio outlet is used to control the final delivery of the coating liquid onto the substrate. The process results in a controlled width layer of coated material on the substrate. The width (track width) is adjustable and is designed into the slot-die outlet. By controlling the rate of solution deposition and the speed of the substrate, thin material coatings in the range of 10 nanometres to hundreds of micrometres can be obtained. Due to its high throughput potential, the slot-die coating is a popular choice for R2R printing applications. The slot-die method facilitates control of three key factors, namely thickness uniformity, coating uniformity and throughput capacity. These relationships are the result of both the quality of the roll and the characteristics of the coating process. Slot-die coating is the best method for producing large quantities of high-quality thin film because the coatings can be applied rapidly, uniformly, and precisely. This process lends itself to the very narrow tolerances required to produce flexible electronics. The thickness of printing process is determined by several factors, the slot aperture size dimensions, the speed of a moving substrate, number of capillary tubes delivering the ink and the solution pressure for coating/printing for full web or single strip respectively. There is a direct relationship between the substrate speed and the film thickness; if the speed is increased, the film thickness decreases and vice versa [10,11].

The intrinsic limits of the specific R2R restrict the performance of flexible electronics produced by slot-die coating. These include accurate control of the substrate gap across the whole slot-die. These inaccuracies manifest themselves in both the width and thickness of the patterned track, especially when printing several consecutive electronic circuits layers because any printing errors related to width or thickness of the strip (i.e., homogeneity and uniformity) would lead to a build up of error and possible ground faults such as short/leakage in the electrical

circuits [12]. Although numerous examples of the successful integration of R2R coated and printed units have been illustrated [13,14], the manufacturing production cost can be further reduced by increasing the printing speed. However, maintaining the quality of printed tracks is still a major difficulty [15].

As a feasible quality control measure, surface inspection must be thoroughly evaluated. Post process contact profilometry methods have been wieldy used for many years [16]. The main drawbacks of using contact methods is that they are post process (off line), they use physical contact with specimen under test, there have a low measurement speed and could cause damage based on the sample type under test. Therefore, this approach is not compatible for in process high-speed and high-volume manufacturing platforms. Due to the extreme difficulty of measuring the surface characterisations of printed tracks optical techniques have been widely used. The present authors have in addition demonstrated Wavelength Scanning Interferometry (WSI) as a viable in process tool for surface metrology [17]. However, one of the limitations is the limited field of view, therefore, surface inspection in real-time is still a challenge. Industry's demand for increased flexibility, productivity, and product quality has necessitated the further development of larger field of view non-contact optical systems [18-20]. Simple camera based optical systems have numerous advantages, including being robust, fast, low cost, capable of monitoring material properties in real-time, and simple to use. Machine vision sensor (MVS) has been implemented to meet embedded metrology requirements for assessments such as surface classification and a high-speed defect detection. MVS was used to measure surface parameters directly for specific parts by detecting the edge profile by using a high-speed CMOS camera and applying an appropriate image processing method to extract the surface profile information [20]. Low levels of printed track width variation and consequent edge straightness indicate print quality. Width and edge variation and functionally affect track electrical resistivity and electrical connectivity of consequent layers as shown in Figure 1.

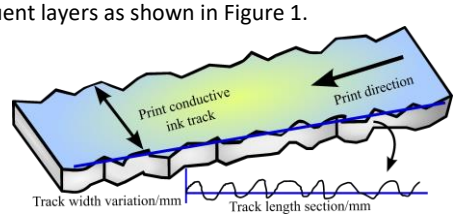

Figure 1. Schematic view of printed tack and track edge.

In this paper, the present authors suggest the use of a MVS for in plane inspection of coating quality and defect detections. This sensor is equipped with a broadband light source in a partially bright field, high-speed cameras, frame grabber linked to a high-performance computer. While the web is static or moving, images are captured and analysed using two image processing methods: the Sobel operator to inspect the coating defects and the Otsu thresholding method to determine and extract the coated inks edge profile. The arithmetic average ($R_{a\ (LAT)}$) has been suggested as a measure of edge irregularity for the printed track, this is the lateral plane equivalent to the (R_a) parameter used in conventional surface metrology. The result of this method is aimed at precise in-process track assessment within the production line and the techniques could be applied to other large area planer applications requiring in-process surface inspection measurements.

2. Principle of Operation

The inspection algorithm's goal is to detect and quantify dimensions and or defects associated with the printed tracks using the MVS. The detection results are analysed for various measuements related to the printing process and can be interrogated to ultimately alert and then manage the production process. In this work, we emphasis the edge line detection for printed tracks and present a method for implementation into automated printed track inspection.

2.1. Edge Detection Method

The detection of the edges may be considered as quantifying border between the measured object (neighbouring regions of uniformity) and its background of the sample. The purpose of using edge detection methods in image processing applications is to reduce the information to be processed while preserving the essential parameters that are directly linked to the shapes of the objects within the image [21]. To apply this method, there are general steps that should be applied sequentially such as filtering, enhancement and the localisation (region of interest-ROI). In this work, the Sobel operator approach has been used to inspect coating quality and detect defects. In comparison with other filtering evaluation methods, the Sobel operator is easier as it mainly determines first-order derivatives using convolution method. The Sobel method has many features such as a high speed of computing time, less amount of data needed for computation, robustness to noise and high accuracy in locating the edge position. A kernel (mask) is important to apply to the original image to overcome false edge detection results. In the present case a (3x3) mask type was utilized for horizontal and vertical real time image gradient directions. These masks can demonstrate as:

$$Sx = \begin{bmatrix} 1 & 0 & -1 \\ 2 & 0 & -2 \\ 1 & 0 & -1 \end{bmatrix}, Sy = \begin{bmatrix} -1 & -2 & -1 \\ 0 & 0 & 0 \\ 1 & 2 & 1 \end{bmatrix} \quad (1)$$

Where *x* and *y* represent the gradient directions respectively; and for the continuous function of the actual position (*x*,*y*) and the first derivative output ($\nabla f(x,y)$) is the gradient of an image at point (*x,y*). Then it can be calculated the gradient direction (θ), more details in [22].

2.2 Evaluation Edge line using Otsu method

Various segmentation techniques have been explored such as line differentiation, automatic and dynamic thresholding [23]. The Otsu approach is a viable automatic threshold selection methods; this type of thresholding approach depends on the frequency distributions of the samples (objects). As a result, the frequency distributions for foreground and background pixels are considered, consequently, finding a threshold value between two class-variance distributions (i.e. two histogram mods). The Otsu method can be represented by 2D grayscale intensity [22, 24]. The pixels set for the entire image is divided into distinct subsets representing background and foreground (e_0 and e_1) respectively. For a threshold q, it is possible to find a combined width for two classes variances (σ_w) from:

$$\sigma_w^2(q) = P_0(q)\sigma_0^2(q) + P_1(q)\sigma_1^2(q) = \frac{1}{MN}[n_0(q)\times\sigma_0^2(q) + n_1(q)\times\sigma_1^2(q)] \quad (2)$$

There are two probabilities $P_0(q)$, $P_1(q)$ for sets e_0 and e_1 respectively. Therefore, the probabilities for both sets can be calculated; more details in [24]. Therefore, the total variance is the sum of the within and between the class variance as:

$$\sigma_T^2 = \sigma_w^2(q) + \sigma_b^2(q) \quad (3)$$

The Otsu method is an effective approach when thresholding images with good distinction between foreground and background; this approach is ideal for images that have a multimodal/ bimodal distribution.

3. Experimental setup

Figure (2.a) shows a fundamental layout of the MVS apparatus. The essential MVS components comprise four parts: lighting arm, printed web (sample under test), capture arm and acquisition process arm. The lighting arm is represented by a broadband light source (HLV3-3M-RGB-4/LED colour) with maximum power (11W), the intensity of the light source can be adjusted based on the selected channel. To capture all sample features, the critical light source parameters including brightness, distance, the angle of light source, web type, intensity, colour, and shape and size of the light source's head have been carefully considered. The main focus of investigation of this work is to detect the edge and edge defects of the printed track hence partial bright field lighting is suggested. This type of light field is widely used in machine vision applications as it is a good option for producing contrast and improving topographical surface details. The broadband light is reflected from the printed web to the capturing arm.

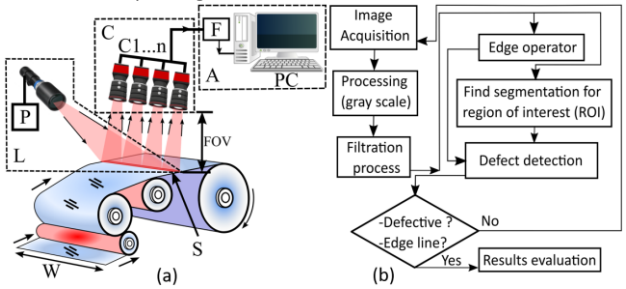

Figure 2. (a) MVS diagram (Keys: L: Lighting arm, L1: Colour light source, P: Power supply, C: Capture arm, C1: Camera/s, A: Acquisition process arm, F: Frame Grabber, S: Scanning range and W: Web, (b) overall flow-chart defect inspection sensor .

The printed web is the subject of the sensor which is represented as the sample under test. The MVS should identify defects and irregularities on the web that can produced during the slot-die process. By acquiring the light intensity reflected form the web, the capture arm (camera/s) monitors variations and unexpected area changes in web features based on the type of printed ink. The sample of the printed web, in this case Silver Ink on Polyethylene Terephthalate (PET) substrate has been used to verify sensor validity. A Baumer camera/s (VCXG-15C.PTP) has been used which has sensor type (SONY IMX273) with resolution (1440 × 1080 pixels/ 1.5 Megapixel) and pixel size (3.45 µm x 3.45 µm). In the present study the camera/s was mounted perpendicular (90º) to the web on a telescope frame (X-Y). The axis movement was adjusted to obtain the correct focus distance during image capture from the web. The light source is positioned at an angle proportional to the cameras. The optical lens type (VS-MC1-160) was fitted to the camera using a C-mount. The exposure time of the camera has been set to be compatible with the web speed. The scanning range, noted here as S (mm), of MVS is number of cameras dependent. The maximum rectangular area can be calculated using a single camera horizontal field of view (H_{FOV}) multiplying by the number of cameras (H_{FOV} X number of cameras) (see Figure 2.a). The S value was calculated using Equation 4 as stated in Table 1.

$$f = \frac{H \times WD}{H_{FOV}} \tag{4}$$

Where f (33.7 mm) is the effective focal length of the optical lens, H is the horizontal sensor size (4.96 mm), WD (60,1 mm) is the work distance of optical lens and H_{FOV} is the horizontal field of view. Practically, sensor calibration is crucial for determining the sensor's resolution (i.e. ability to determine the smallest distance between objects (line pairs per millimetre (lp/mm)). By utilising standard resolution test targets (R3L3S1N Negative, 1951 USAF Targets, Thorlabs) the resolution (R) of the sensor has been calculated based on lens (VS-MC1-160) parameters and by applying Equation (5). The sensor can be resolved group 7 and elements 3.

$$R\,(Line\,pair\,/\,mm) = 2^{Group+(\frac{Element-1}{6})} \tag{5}$$

It is vital to note that the scanning range is inversely proportional to the sensor magnification (i.e., this yields low sensor resolution). The results are illustrated in table (1).

Table 1 (Horizontal and vertical field of view, resulstion and scanning range of the sensor)

Lens type	H_{FOV} (mm)	V_{FOV} (mm)	R (μm)	S (mm)
VS-MC1-160	8.84	6.63	6.16	8.84

In this work, we aim to evaluate the straightness of the print track. We, therefore, introduce the parameter $R_{a(LAT)}$. The average roughness of a surface (R_a, the arithmetic mean) is wieldy used to calculate the vertical height deviation [25]. The R_a is evaluated as:

$$R_a = \frac{1}{L}\int_0^L |Z(x)dx| \tag{6}$$

The $Z(x)$ is the surface height along the profile length. Instead of using the vertical deviation, $R_{a(LAT)}$ uses the lateral deviation of the edge of the printed ink line, see Figure 1, to compute the straightness of the print track over the assessed length (L). This parameter has a functional significance in terms of track resistivity and overall track positioning. The parameter is computed as the mean variation from the fitted mean line of the track edge, where the ink edge is detected by the image analysis tool.

4. Experimental results

In the current approach, the authors examine the performance and validity of the MVS for measuring the ink defect/edge-line on the web. To illustrate the measurement capability of MVS the results are compared to a static measurement (Leica MZ6 digital Microscope) of the printed web used for the MVS analysis. The web sample tested was a silver based ink on a PET (Polyethylene Terephthalate) substrate. The border line (edge-line) between two areas background web surface (PET) and silver ink was used to investigate the efficacy of the approach. The MVS successfully inspected web sample by integrating both the Sobel operator to inspect coating quality of the sample under test and Otsu approach to retrieve the ink edge profile. As shown in Figure 3.a, b, the magnitude variation can indicate that there are two different surface types (i.e. bare substrate surface vs silver ink area). This can be used for edge/defect detection.

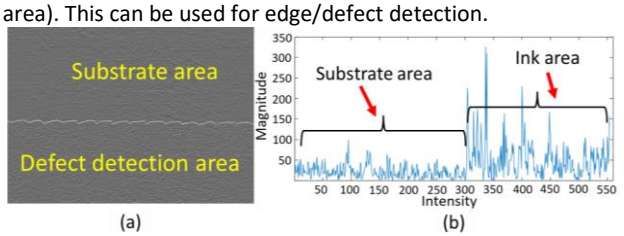

Figure 3. Silver Ink on Polyethylene Terephthalate (PET) substrate (a) Sobel operator output, (b) cross-section intensity profile.

In Figure 4.a, b, the edge profile has been extracted by using Otsu method in MountainMap software. The $R_{a(LAT)}$ has been calculated using equation (6). The $R_{a(LAT)}$ value was found to be 0.4 µm. To investigate the system performance at real-time, the same sample was placed on roll-to-roll demonstrator rig and moved at speed 1m/min. The acquisition time was set to be 79 frame per second. The $R_{a(LAT)}$ at dynamic situation was found to

be 0.5 µm. As such, there is 0.1 µm measurement deviation between the static and dynamic operations.

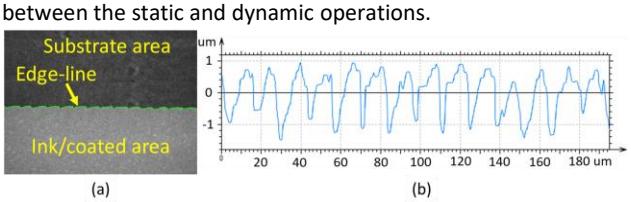

Figure 4. Silver Ink on Polyethylene Terephthalate (PET) substrate (a) Otsu output, (b) Extracted edge profile.

5. Conclusions:

To inspect printed web quality a high-speed MVS, was used to detect ink edge quality. By applying the MVS method, it is possible to measure the web quality accurately and quickly. It widely predicted that the consumption of printed electronics will further increase in the future, and a high-quality print is required for producing high-quality devices. Therefore, a high-speed inspection MVS will be useful in ensuring the production of high-quality prints where the data can be used as feedback for process control. This in plane measurement approach can be integrated with other sensor approaches such as out of plane thickness measurements or surface chemistry to facilitate AI assisted approached to be developed for R2R device production.

In the present work the Sobel operator has been used to evaluate printing quality and identify any defects. The image segmentation algorithm based on the Otsu's thresholding method has been applied to define and extract the ink's edge line. For the silver ink on PET substrate used in the present study, the parameter $R_{a\,(LAT)}$, represents the edge line straightness. The $R_{a\,(LAT)}$ is calculated from the captured web images and was found to be 0.4µm and 0.51µm for static and dynamic measurements respectively. However, there are some limitations to using MVS for R2R assessments and these limitations should be considered at the initial design, for instances, it has a limited capture area based on FOV of the lens utilised, types and number of cameras sensor, type of illumination of the light source, performance of the PC hardware's (i.e., processing time). Nonetheless, MVS is a useful instrument for dynamic inspection of web quality. With multiple measurement MVS stations in parallel providing a comprehensive solution for R2R applications.

Acknowledgments

The authors would like to acknowledge funding EPSRC Responsive Manufacturing funding (EP/V051261/1) for this work and funding for foreground research from The ESPRC Future Manufacturing Hub (EP/P006930/1).

References

[1] Lee, J., Byeon, J., & Lee, C. (2020). Theories and control technologies for web handling in the roll-to-roll manufacturing process. *International Journal of Precision Engineering and Manufacturing-Green Technology*, **7**(2), 525-544.

[2] Thi, L. T., Tung, L. N., Thanh, C. D., Quang, D. N., & Van, Q. N. (2019, July). Tension regulation of roll-to-roll systems with flexible couplings. In 2019 *International Conference on System Science and Engineering (ICSSE)* (pp. 441-444). IEEE.

[3] Carvalho, M. S., & Kheshgi, H. S. (2000). Low-flow limit in slot coating: Theory and experiments. *AIChE journal*, **46**(10), 1907-1917.

[4] Romero, O. J., & Carvalho, M. S. (2008). Response of slot coating flows to periodic disturbances. *Chemical Engineering Science*, **63**(8), 2161-2173.

[5] Yang, J., Vak, D., Clark, N., Subbiah, J., Wong, W. W., Jones, D. J., ... & Wilson, G. (2013). Organic photovoltaic modules fabricated by an industrial gravure printing proofer. *Solar Energy Materials and Solar Cells,* **109**, 47-55.

[6] Liu, F., Ferdous, S., Schaible, E., Hexemer, A., Church, M., Ding, X., ... & Russell, T. P. (2015). Fast printing and in situ morphology observation of organic photovoltaics using slot-die coating. *Advanced materials*, **27**(5), 886-891.

[7] Ro, H. W., Downing, J. M., Engmann, S., Herzing, A. A., DeLongchamp, D. M., Richter, L. J., ... & Yan, H. (2016). Morphology changes upon scaling a high-efficiency, solution-processed solar cell. *Energy & Environmental Science*, **9**(9), 2835-2846.

[8] Hong, S., Kang, H., Kim, G., Lee, S., Kim, S., Lee, J. H., ... & Lee, K. (2016). A series connection architecture for large-area organic photovoltaic modules with a 7.5% module efficiency. *Nature communications*, **7**(1), 1-6.

[9] Maisch, P., Tam, K. C., Schilinsky, P., Egelhaaf, H. J., & Brabec, C. J. (2018). Shy organic photovoltaics: digitally printed organic solar modules with hidden interconnects. *Solar RRL*, **2**(7), 1800005.

[10] Romero, O. J., Suszynski, W. J., Scriven, L. E., & Carvalho, M. S. (2004). Low-flow limit in slot coating of dilute solutions of high molecular weight polymer. *Journal of Non-Newtonian Fluid Mechanics,* **118**(2-3), 137-156.

[11] Stephane et al., H. (2016). Solar trees: first large-scale demonstration of fully solution coated, semitransparent, flexible organic photovoltaic modules. *Advanced Science*, **3**(5), 1500342.

[12] Bajaj, M., Prakash, J. R., & Pasquali, M. (2008). A computational study of the effect of viscoelasticity on slot coating flow of dilute polymer solutions. *Journal of non-newtonian fluid mechanics*, **149**(1-3), 104-123.

[13] Mohanty, D., Li, J., Born, R., Maxey, L. C., Dinwiddie, R. B., Daniel, C., & Wood III, D. L. (2014). Non-destructive evaluation of slot-die-coated lithium secondary battery electrodes by in-line laser caliper and IR thermography methods. *Analytical Methods*, **6**(3), 674-683.

[14] Välimäki, M., Apilo, P., Po, R., Jansson, E., Bernardi, A., Ylikunnari, M., ... & Hast, J. (2015). R2R-printed inverted OPV modules–towards arbitrary patterned designs. *Nanoscale*, **7**(21), 9570-9580.

[15] Krebs, F. C., Fyenbo, J., Tanenbaum, D. M., Gevorgyan, S. A., Andriessen, R., van Remoortere, B., ... & Jørgensen, M. (2011). The OE-A OPV demonstrator anno domini 2011. *Energy & Environmental Science,* **4**(10), 4116-4123.

[16] Magonov, S. N., & Whangbo, M. H. (1996). *Surface Analysis with STM and AFM.* VCH.

[17] Muhamedsalih, H., Blunt, L., Martin, H., Hamersma, I., Elrawemi, M., & Feng, G. (2015). An integrated opto-mechanical measurement system for in-process defect measurement on a roll-to-roll process. euspen.

[18] Hassan, M. A., Martin, H., & Jiang, X. (2014). Surface profile measurement using spatially dispersed short coherence interferometry. *Surface Topography: Metrology and Properties*, **2**(2), 024001.

[19] Gao, F., Muhamedsalih, H., Tang, D., Elrawemi, M., Blunt, L., Jiang, X., ... & Hollis, P. (2015, August). In-situ defect detection systems for R2R flexible PV barrier films. In 2015 International Conference on Optical Instruments and Technology: O*ptoelectronic Imaging and Processing Technology* (**Vol. 9622**, pp. 93-101). SPIE.

[20] Gao, Z., & Zhao, X. (2012). Roughness measurement of moving weak-scattering surface by dynamic speckle image. *Optics and Lasers in Engineering*, **50**(5), 668-677.

[21] Sun, Q., Hou, Y., Tan, Q., Li, C., & Liu, M. (2014). A robust edge detection method with sub-pixel accuracy. *Optik*, **125**(14), 3449-3453.

[22] Hernandez, M. E., Villalobos, J. R., & Johnson, W. C. (1993, August). Sequential computer algorithms for printed circuit board inspection. In Intelligent Robots and Computer Vision XII: Active Vision and 3D Methods , Vol. **2056**, pp. 438-449. SPIE.

[23] Otsu, N. (1979). A threshold selection method from gray-level histograms. *IEEE transactions on systems, man, and cybernetics*, **9**(1), 62-66.

[24] Burger, W. and M.J. Burge, Digital Image Processing: An Algorithmic Introduction. 2022: *Springer International Publishing*.

[25] Whitehouse, D. J. Surfaces and their Measurement. *Butterworth-Heinemann (2012)*.